Supporting Information

A High-Temperature Continuous Stirred-Tank Reactor Cascade for the Multistep Synthesis of InP/ZnS Quantum Dots

Ioannis Lignos, [a] *Yiming Mo,* [a] *Loukas Carayannopoulos,* [a] *Matthias Ginterseder,* [b] *Moungi G. Bawendi,* [b] *and Klavs F. Jensen* [a*]

[a] Department of Chemical Engineering, Massachusetts Institute of Technology, 77 Massachusetts Avenue, Cambridge, MA 02139, U.S.A

[b] Department of Chemistry, Massachusetts Institute of Technology, 77 Massachusetts Avenue, Cambridge, MA 02139, U.S.A

[*] kfjensen@mit.edu

Contents

Materials & Methods

Materials

Indium(III) chloride (99.999%), zinc(II) chloride (≥98%), zinc(II) iodide (≥98%), tris(diethylamino)phosphine (97%), selenium powder 100 mesh (99.99%), oleylamine (70%), 1-trioctylphosphine (90%), 1-octadecene (90%), ethanol (200 proof, anhydrous, ≥99.5%), hexane (anhydrous, 95%) were purchased from Sigma-Aldrich. Sulfur powder was purchased from Strem Chemicals.

Preparation of precursors

All metal halide solutions were prepared under inert atmosphere. For the preparation of the precursors solutions, 330 mg of indium(III) chloride and 660 mg of zinc(II) chloride were loaded into a 50 mL flask along with 30 mL of oleylamine. In addition, 1200 mg of zinc(II) iodide were loaded in another 50 mL flask along with 30 mL of oleylamine. Both solutions were degassed for 1 hr at 120 °C under N_2. After 1 hr, both solutions were cooled and transferred into 30 mL syringes for further use in the flow experiments. Separately, inside a glove box, 5 mL of tris(diethylamino)phosphine were loaded into a glass syringe. In addition, 1200 mg of S were dissolved in 20 mL TOP and sonicated till the powder was dissolved. The precursor solution was then loaded into a 30 mL syringe.

Particle Purification

For particle purification, 2 mL of crude QD solutions were mixed with 2 mL of ethanol for the precipitation of QDs. After centrifugation, the supernatant was discarded. Finally, the QDs were dissolved in 500 µL of hexane for further characterization.

Offline characterization - instrumentation

Absorption spectra were recorded on a Cary 5000 UV–vis–NIR spectrophotometer. PL spectra were recorded on a Fluoromax 3 fluorimeter. PL QYs were obtained using an integrating sphere (Labsphere, RTC-060- SF) setup. The samples were excited with a 405 nm diode laser (Thorlabs, Compact Laser Diode Module with Shutter, 405 nm, 4.0 mW) chopped at 210 Hz using an optical chopper, and the output was recorded with a calibrated optical power detector, UV Silicon, 200-1100nm, DB15 Calibration Module (818-UV/DB from Newport) using a lock-in amplifier (Stanford Research Systems). The samples were contained in a PTFE-capped quartz cuvette. A solvent blank was used in conjunction with a colored glass longpass filter (Colored-Glass, 2x2 in., 435 nm Cut-on, Model: 20CGA-435 from Newport) blocking the excitation beam to allow correction of the obtained PLQY values for leakage of the excitation light and transmittance of the filter. Additionally, the measured photocurrent was adjusted for the external quantum efficiency of the photodetector. Transmission electron micrographs were recorded using a JEOL 2010 transmission electron microscope operating at 200 kV.

Reactor design

A single CSTR unit consists of three main components, including a high-intensity motor, a stainless-steel block and a stainless-steel cover (Figure 1a). The high-intensity motor consists of a round-face motor (Compact Round-Face DC Motor, 12V DC, 5782 rpm @ 0.81 in. -oz, 6331K21) and an aluminum holder with two neodymium magnets (Neodymium Magnet, Magnetized Through Thickness, 3/8" Thick, 3/8" OD, 5862K123), which provides the magnetic coupling force to spin the stir bar. The stir bar (3/8" diameter, 3/16" height, 3/8" length, VWR Spinplus Magnetic Stir Bar, 58947-820) is located inside the stainless-steel block. The speed of the rotation can be

controlled individually by adjusting the voltage applied to the motor. The stainless-steel reactor is a 1.2” × 1.2” square block with a thickness of 0.54”. The cylinder-shaped inner chamber has a diameter of 0.6” and a depth of 0.28”. An O-ring gap surrounds the chamber for the 1/16’’ Kalrez O-ring (Super-Resilient Kalrez, McMaster Carr, 7075), which was used for sealing. The glass cover is heat-resistant borosilicate glass (Pyrex) with dimensions of 1.2” × 1.2” × 0.187”. The stainless-steel cover is super-corrosion-resistant 316 stainless steel with dimensions of 1.2” × 1.2” × 0.125”. All extruded 2D shapes were fabricated using water jet machining (OMAX MicroMAX JetMachining Center). In addition to 2D shapes, the reactor chamber and the O-ring gap were machined using CNC milling (ProtoTRAK SMX). Multiple CSTR units are connected using stainless steel sample loops (VWR, 50806-950) and they are mounted on an aluminum 80/20 framing holder (Fig. 1b). The aluminum holder (1.2” × 1.2” × 18”) can hold up to 8 CSTRs. The holder is attached on a peristaltic pump (Masterflex L/N peristaltic pump HV-77919-35) to allow for automatic rotation of the platform (vertical or horizontal orientation) depending on the experimental needs. All connection ports have 1/4-28 threads, which can be directly connected using common IDEX fittings (IDEX Health & Science LLC.) without additional adapters. For the temperature control of each unit, Watlow EZ Zone RM PID controllers (RMHF-11CC-A1AA, IES Technical Sales) were used, and the temperature of each unit was adjusted via a custom Labview Program. All electronics were combined in to one control tower, which was shielded from hazardous chemical reagents with a polycarbonate cover. During synthesis, six syringe pumps (Harvard Apparatus PHD 2000 Dual Syringe Pumps) were utilized for solution injection. All pumps were controlled via a custom Labview Program.

In-line absorbance and fluorescence analysis

A flow cell was integrated at the outlet of the cascade for in-line detection of the formed QDs *via* in-situ absorption and fluorescence spectroscopy (light source: Ocean Optics, Inc., DH-2000-BAL; spectrometer: Ocean Optics, Inc., HR2000+). The flow cell is an aluminum block with inlet and outlet ports (1/4-28 threads, which can be directly connected using common IDEX fittings) and three ports which can be connected using optical fibers (see Fig. S1). The customized flow cell can be used for both absorbance and photoluminescence measurements. The spectrometer was operated between 350 and 1100 nm, and data recorded using 100-500 ms integration times using a custom Labview Program. In order to properly process the raw data, several background spectra were collected. A dark spectrum, with the light source shutter closed, as well as a solvent spectrum were taken first. These spectra must be subtracted from the sample when calculating the absorbance. Product solutions were also collected for particle purification and additional offline characterization.

Residence time distribution (RTD) measurements

The RTD profiles of the CSTR cascade, were obtained using the pulse injection method. The carrier phase was deionized (DI) water, and the tracer was methylene blue. In-line UV-Vis spectroscopy (using the optical system, which was described in the previous section) was used to determine the concentration profiles of the tracer at the inlet and outlet. A six-way valve (IDEX Health & Science LLC., MXP7900-000) combined with LabVIEW control enabled automatic pulse injection and data collection (see Figure S2 for a schematic of the experimental setup).

Figures

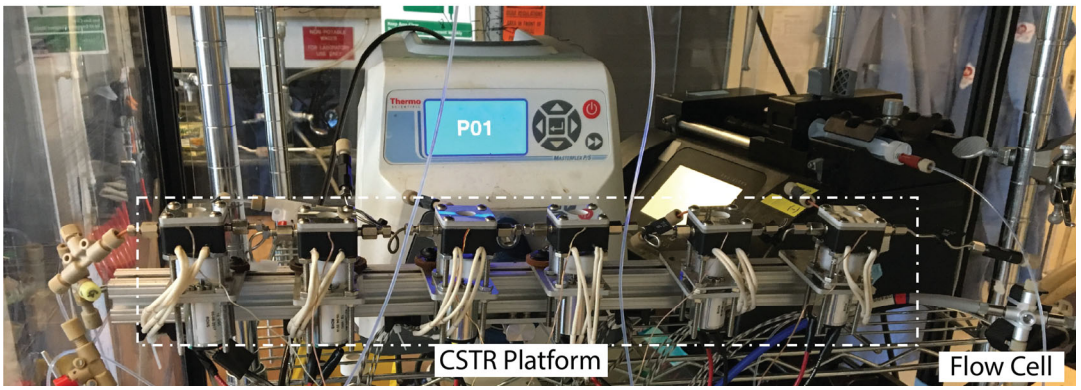

Figure S1: Image of the high-temperature continuous stirred-tank reactors for the synthesis of InP/ZnS QDs

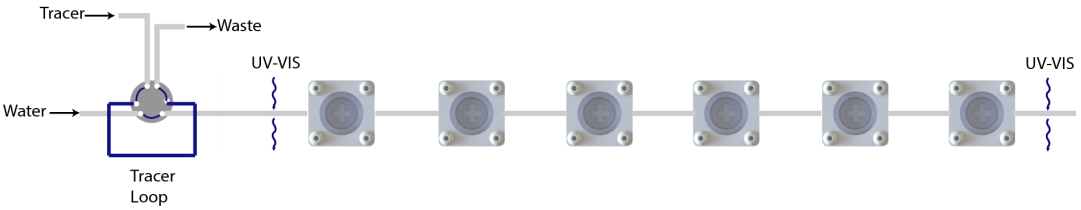

Figure S2: Scheme of the residence time distribution measurements using in-line UV-Vis to record concentration profiles at the inlet and outlet**.**

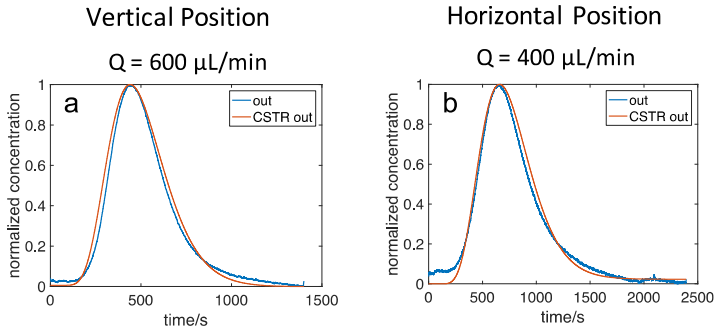

Figure S3: RTD profiles of the high-temperature CSTR cascade when the orientation is (a) vertical and (b) horizontal. Blue line is the experimental RTD profile and the red line represents the profile based on the ideal CSTRs in series model.

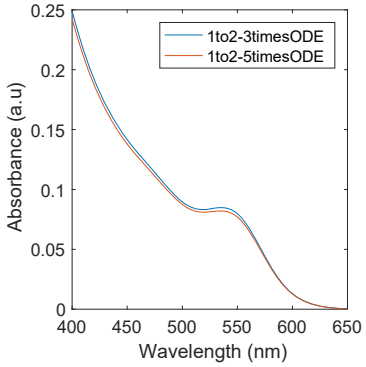

Figure S4: Absorbance spectra of InP QDs with a 2-times decrease of precursor concentrations and 5-times dilution of the aminophosphine precursor with octadecene

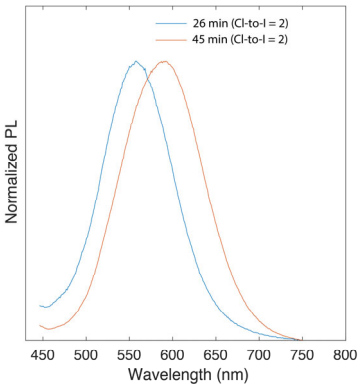

Figure S5: PL spectra of the synthesized core-shell QDs (for two different reaction times), when the platform was fixed at a horizontal orientation. The emission linewidths of the synthesized QDs were in the range of 90-100 nm, which were broader compared to the emission linewidths using the vertical orientation.

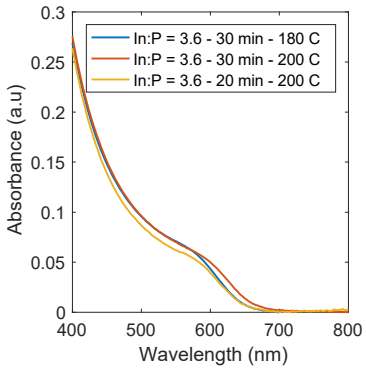

Figure S6: Absorbance spectra of InP QDs at different temperatures and reaction times at a constant In:P molar ratio.

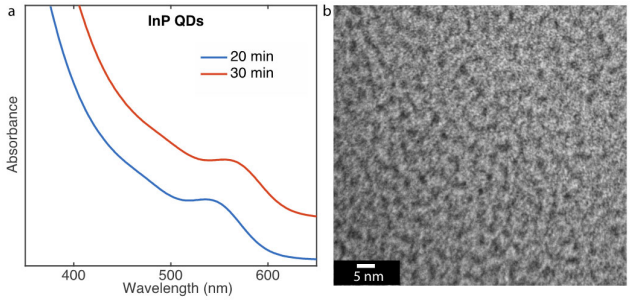

Figure S7: (a) Absorption spectra of InP QDs after 20 and 30 min of reaction. Other parameters were fixed: T = 180 °C, In-to-P = 3.6, (b) A transmission electron microscopy image of the synthesized InP QDs.

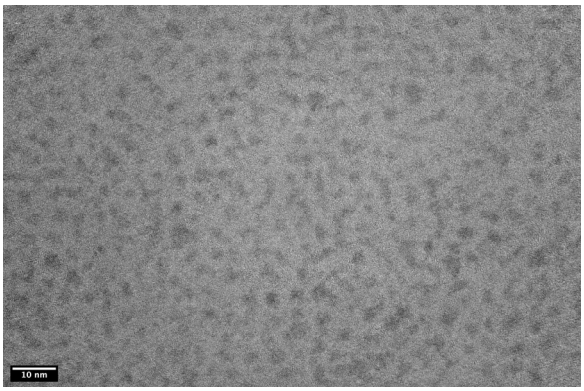

Figure S8: A transmission electron microscopy image of the synthesized InP QDs. The reaction time for the growth of InP QDs was 13 min for the shell growth 15 min. Other parameters were fixed: T_{core} = 180 °C, T_{shell} = 290 °C, In-to-P = 3.6, S-to-Zn = 2 and Cl-to-I = 6.

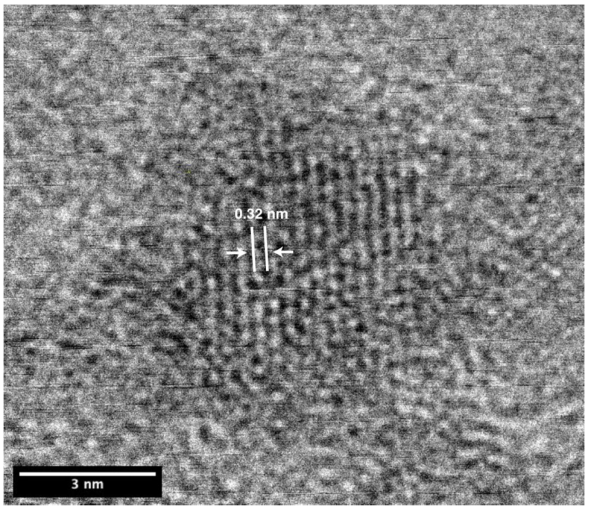

Figure S9: High-resolution transmission electron microscopy image of InP/ZnS QDs. Lattice fringes of InP/ZnS QDs shown to be 0.32 nm.

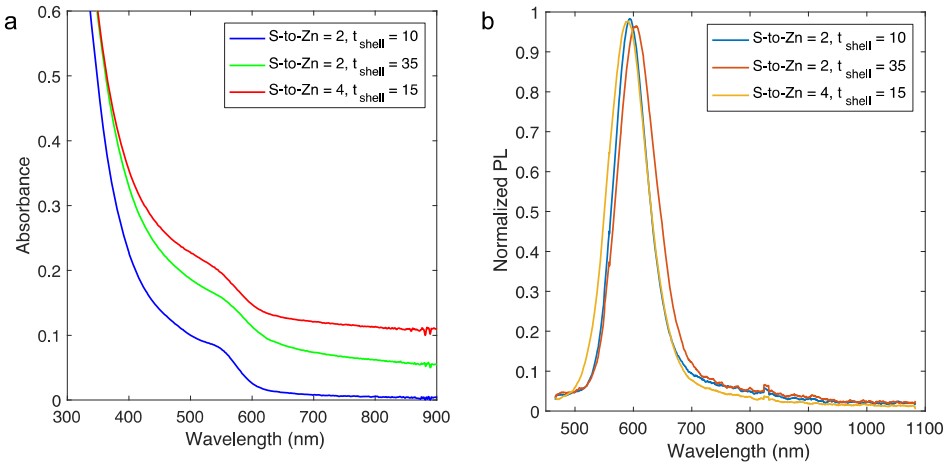

Figure S10: (a) Absorbance and (b) PL spectra of InP/ZnS quantum dots for different S-to-Zn molar ratios and at different shell formation times. The shell formation temperature was set at 260 °C.

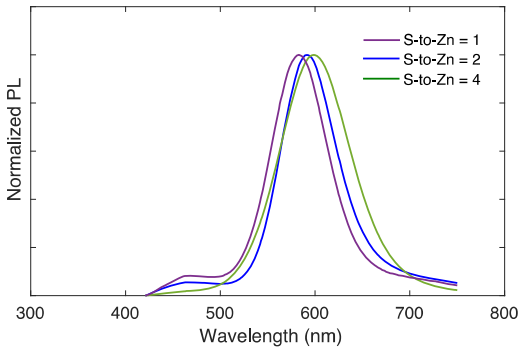

Figure S11: PL spectra of InP/ZnS quantum dots for different S-to-Zn molar ratios and at different shell formation times. The shell formation temperature was set at 280 °C.

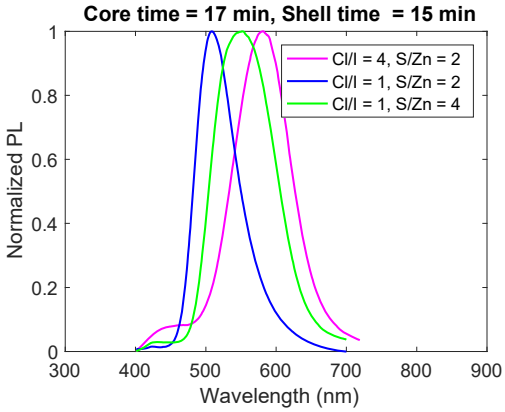

Figure S12: PL spectra of InP/ZnS quantum dots for different S-to-Zn and Cl-to-I molar ratios with fixed times and temperatures. The shell formation temperature was set at 290 °C.

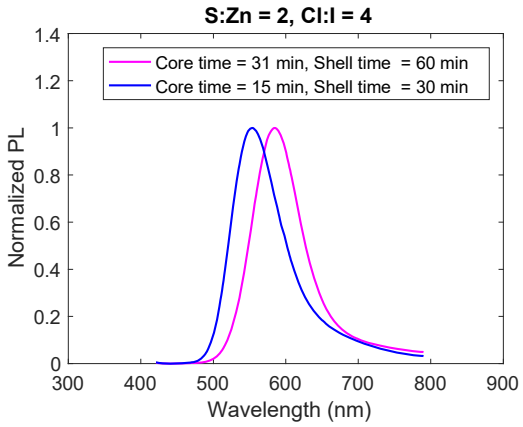

Figure S13: PL spectra of InP/ZnS quantum dots for different reaction times at various S-to-Zn and Cl-to-I. The shell formation temperature was set at 290 °C.

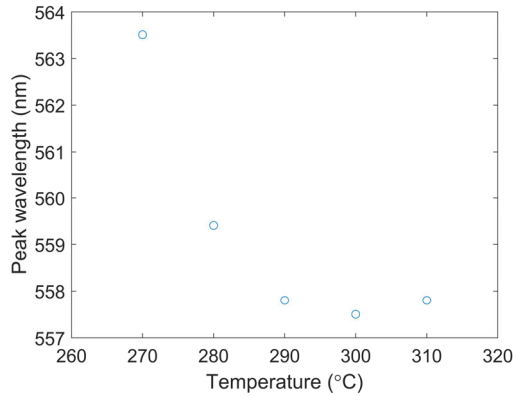

Figure S14: PL peak change by changing the shell formation temperature. Reaction conditions correspond to those used in Figure 4.